NEW YORK UNIVERSITY
INSTITUTE OF MATHEMATICAL SCIENCES
LIBRARY
25 Waverly Place New York 3, N.Y.

NYO 7696

AEC Computing Facility

AEC RESEARCH AND DEVELOPMENT REPORT

PHYSICS

NYO-7696

A NUMERICAL METHOD FOR THE TIME-DEPENDENT TRANSPORT EQUATION

by

R. D. Richtmyer

February 1957

institute of mathematical sciences

NEW YORK UNIVERSITY

NEW YORK, NEW YORK

This report was prepared as an account of Government sponsored work. Neither the United States, nor the Commission, nor any person acting on behalf of the Commission:

A. Makes any warranty or representation, express or implied, with respect to the accuracy, completeness, or usefulness of the information contained in this report, or that the use of any information, apparatus, method, or process disclosed in this report may not infringe privately owned rights; or

B. Assumes any liabilities with respect to the use of, or for damages resulting from the use of any information, apparatus, method, or process disclosed in this report.

As used in the above, "person acting on behalf of the Commission" includes any employee or contractor of the Commission to the extent that such employee or contractor prepares, handles or distributes, or provides access to, any information pursuant to his employment or contract with the Commission.

AEC Computing Facility
Institute of Mathematical Sciences
New York University

PHYSICS NYO-7696

A NUMERICAL METHOD FOR THE TIME-DEPENDENT TRANSPORT EQUATION

by

R. D. Richtmyer

February 1957

Contract No. AT(30-1)-1480

A NUMERICAL METHOD FOR THE TIME-DEPENDENT TRANSPORT EQUATION

by

R. D. Richtmyer

ABSTRACT

A finite difference method has been devised for the numerical solution of the integro-differential equation of neutron transport in a sphere. The method is applied here to one-group problems with isotropic scattering, although some degree of generalization is possible. Special features of the method include integration of the equations along the neutron trajectories in space-time and special treatment of exceptional net points which lie near the boundary of the relevant region of phase space. The method is the outcome of a series of investigations initiated by a suggestion of Von Neumann in 1948.

Numerical tests of the method, made with the Univac at New York University, are described. They deal with the problem of a homogeneous bare sphere subject to a singular initial condition. In connection with those tests, codes were divised to provide accurate numerical integration of the integral equation for the normal mode functions.

A NUMERICAL METHOD FOR THE TIME-DEPENDENT TRANSPORT EQUATION

TABLE OF CONTENTS

A NUMERICAL METHOD FOR THE TIME-DEPENDENT TRANSPORT EQUATION

I. Introduction

A finite difference method for solving the time-dependent transport equation in spherical systems was devised by John Von Neumann, Herman H. Goldstine and the writer (unpublished) in 1948 in connection with work of the Los Alamos Scientific Laboratory and was used in extensive machine calculations in 1949 and 1950. The essential feature of the method was the use of the quasi-cartesian coordinates described below. In 1952 and 1953 the method was further improved and simplified by integrating along the neutron trajectories in space-time; preliminary tests of the method (unpublished) in this form were made on the Los Alamos computer ("Maniac"). During the past year and a half further tests have been made on the Univac at New York University for a simplified problem and during the course of these tests some further substantial improvements of the method have been devised, to provide more accurate treatment of exceptional net points near the boundary of the system.

The latest version of the method and the Univac tests will be described here.

For practical problems the time-dependent version of Carlson's S_n method has been generally preferred in recent work, because of its smaller demands on machine speed and capacity; but the method presented in the present report is of interest because of its directness and simplicity.

II. The Initial Value Problem

To simplify discussion, attention will be confined to the simplest possible version of the problem by making the following assumptions:

1. All neutrons have the same speed ("one-group treatment").
2. Scattering is isotropic.
3. Cross-sections and other material parameters are time-independent.

It will probably be obvious to the reader that some degree of generalization is possible and necessary for practical problems.

Let r = radial coordinate; μ = cosine of the angle between the radius vector and the velocity vector; t = time; v = neutron speed; $\sigma = \sigma(r)$ = collision probability per unit path length (also called the macroscopic cross-section or inverse mean free path); $1 + f = 1 + f(r)$ = average number of neutrons emerging from a collision, by scattering and fission; $\psi(r,\mu,t)$ = number of neutrons at time t per unit volume of space at position r per unit solid angle about direction μ. Then the transport equation is

$$\left(\frac{1}{v}\frac{\partial}{\partial t} + \mu\frac{\partial}{\partial r} + \frac{1-\mu^2}{r}\frac{\partial}{\partial \mu} + \sigma\right)\psi(r,\mu,t)$$

$$= \sigma\frac{1+f}{2}\int_{-1}^{1} d\mu'\psi(r,\mu',t). \qquad (1)$$

This equations is to be satisfied for $0 \leq r \leq a$, $-1 \leq \mu \leq 1$, $0 \leq t$, where a is the (outside) radius of the system; the equation is to be taken together with an initial condition:

$$(2) \qquad \psi(r,\mu,0) = \psi_o(r,\mu) \quad \text{(given)},$$

and a boundary condition:

$$(3) \qquad \psi(a,\mu,t) = 0 \quad \text{for} \quad -1 < \mu < 0.$$

If the reader so desires, he may regard the requirement that all terms of (1) be bounded as $r \to 0$ as an additional boundary condition holding at $r = 0$.

Many properties of this initial value problem are well-known, at least if the functions $\sigma(r)$ and $f(r)$ are sufficiently well-behaved -- for example piecewise continuous*. Some of these properties are:

1. A unique solution exists for $t \geq 0$ if the initial function $\psi_o(r,\mu)$ is piecewise continuous.
2. The solution depends continuously on the initial function in the sense of the maximum norm.
3. The solution cannot grow faster than at a certain exponential rate, namely:

$$(4) \qquad |\psi(r,\mu,t)| \leq e^{Bt} \max_{\substack{0\leq r\leq a \\ -1\leq\mu\leq 1}} |\psi_o(r,\mu)|$$

*Piecewise continuity is taken to include possession of one-sided limits at each discontinuity, hence boundedness.

where

$$B = v[\underset{o\leq r\leq a}{\text{Max}}\ \sigma(r)]\ [\underset{o\leq r\leq a}{\text{Max}}\ f(r)]$$

4. The solution is continuous in r and μ for $t > 2a/v$ even if the initial function is discontinuous.

5. The general solution of the initial value problem can be expressed in terms of normal mode solutions and a residuum as follows:

$$(5)\qquad \psi(r,\mu,t) = \sum_{(n)} A_n \psi^{(n)}(r,\mu)e^{\alpha^{(n)}t} + d(r,\mu,t)$$

where, for each $n = 0,1,2,\ldots$, $\alpha^{(n)}$ and $\psi^{(n)}$ are a constant and a function characterizing the n^{th} normal mode; the constants A_n and the residuum $d(r,\mu,t)$ depend on the initial function but in any case can be so chosen that as $t \longrightarrow \infty$, $d(r,\mu,t)$ decreases faster than any normal mode.

(This last is a conjecture based on the studies of homogeneous bare slabs and spheres by Lehner and Wing -- see article by Lehner in Communications on Pure and Applied Mathematics, vol. IX, 1956. For the slab the summation in (5) is a finite one and the residual term is generally necessary. For spherical systems the summation is probably an infinite one and the residual term may not be necessary.)

Clearly this initial value problem is suitable for attempts at numerical solution.

III. The Quasi-Cartesian Coordinates

In place of r, ϑ, we take as independent variables the quantities

$$(6) \qquad \begin{aligned} x &= r\mu = r\cos\vartheta, \\ y &= r\sqrt{1-\mu^2} = r\sin\vartheta, \end{aligned}$$

where we have written $\mu = \cos\vartheta$.

These are not cartesian coordinates in the ordinary sense because r and ϑ are not polar coordinates in the ordinary sense. ϑ is the angle between the radius vector and a fixed direction. In terms of the straight line on which a neutron is moving at time t, y is the shortest distance from this line to the origin and x is the distance along this line measured from the point nearest the origin to the present position of the neutron, the positive direction being taken as that of the neutron's motion. Thus, x and y are cartesian coordinates in a plane which shifts its orientation abruptly when there is a collision.

With these variables, and calling $\Psi(x,y,t) = \psi(r,\cos\vartheta,t)$ the transport equation becomes

$$(7) \qquad \left(\frac{1}{v}\frac{\partial}{\partial t} + \frac{\partial}{\partial x} + \sigma\right)\Psi(x,y,t) = \sigma\,\frac{1+f}{4\pi}\,\Phi\left(\sqrt{x^2+y^2},t\right),$$

where $\Phi(r,t)$ is the spatial density given by

$$(8) \qquad \Phi(r,t) = 2\pi\int_0^\pi \Psi(r\cos\vartheta,\ r\sin\vartheta,t)\sin\vartheta\,d\vartheta$$

or

$$(9) \qquad \Phi(r,t) = \frac{2\pi}{r} \int_{-r}^{r} dx\, \Psi(x, \sqrt{r^2-x^2}\,, t).$$

(7) is to be satisfied for $x^2 + y^2 \leq a^2$, $y \geq 0$, $t \geq 0$; the initial condition is

$$\Psi(x,y,o) \text{ given}, \quad x^2 + y^2 \leq a^2, \quad y \geq 0;$$

the boundary condition is

$$(10) \qquad \Psi(x,y,t) = 0 \quad \text{for} \quad x^2 + y^2 = a^2, \quad x < 0, \quad y > 0$$

or

$$\Psi(-\sqrt{a^2-y^2}\,, y, t) = 0 \quad \text{for} \quad 0 \leq y < a.$$

There is no boundary condition at the origin.

The transport equation holds in the shaded semicircular region of figure 1 and the path of integration in

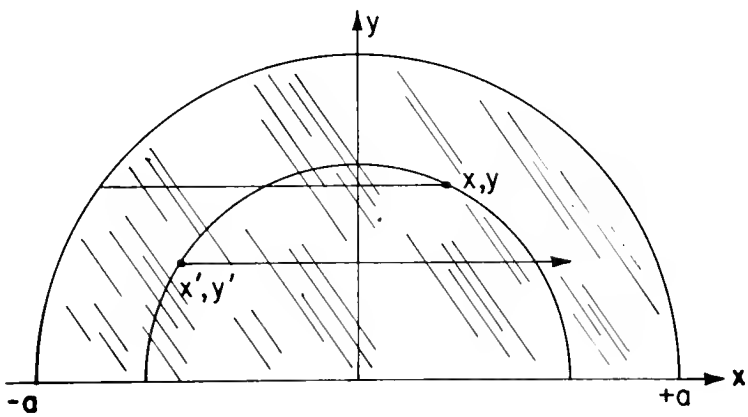

Figure 1

(8) or (9) is a semicircular arc passing through the point x,y. In this figure the point representing a neutron moves

horizontally to the right with speed v until a collision occurs, at which time it jumps to some other point on the same semicircle (say $x'y'$) from which it then continues to move horizontally with speed v. If a neutron escapes from the system it does so by crossing the right-hand quarter circle of the boundary. The boundary condition of no incident flux is that $\Psi = 0$ on the left-hand quarter circle of the boundary.

IV. The Difference Equations

A rectangular net of points in the x,y,t space is chosen by defining

$$x_i = i\Delta x \qquad i = -I,-I+1,\cdots,0,1,\cdots,I$$
$$y_j = j\Delta y \qquad j = 0,1,\cdots,J$$
$$t^n = n\Delta t \qquad n = 0,1,\cdots$$

where the intervals are supposed so chosen that $v\Delta t = \Delta x$ and $I\Delta x = J\Delta y = a$. $\Psi(x_i,y_j,t^n)$ will be denoted by $\Psi^n_{i,j}$. $\Phi(r,t^n)$ will be denoted by $\Phi^n(r)$. Furthermore an interval Δr is chosen for tabulation of $\Phi^n(r)$ and we will denote $\Phi^n(p\Delta r)$ by Φ^n_p. We also denote $\sqrt{x_i^2+y_j^2}$ by $r_{i,j}$. Fractional indices will also be used where convenient.

Because of the relation $v\Delta t = \Delta x$, the space-time point (x_{i+1},y_j,t^{n+1}) lies on the same trajectory* as the point (x_i,y_j,t^n), and we can approximate the derivative terms by writing

$$\left[\left(\frac{1}{v}\frac{\partial}{\partial t} + \frac{\partial}{\partial x}\right)\Psi\right]_{(x_{i+1/2},y_j,t^{n+1/2})} =$$

$$= \frac{\Psi^{n+1}_{i+1,j} - \Psi^n_{i,j}}{\Delta x} + \mathcal{O}((\Delta t)^2) \quad ,$$

and the transport equation is approximated as

---

*The trajectories or characteristics are the lines $x - vt = \text{constant}$, $y = \text{constant}$.

$$\frac{\Psi^{n+1}_{i+1,j} - \Psi^{n}_{i,j}}{\Delta x} + \sigma \frac{\Psi^{n+1}_{i+1,j} + \Psi^{n}_{i,j}}{2} =$$

(11)

$$= \sigma \frac{1+f}{4\pi} \Phi^{n+1/2}(r_{i+1/2,j}) \quad ,$$

where $\Phi^{n+1/2}(r)$ is an approximate value of $\Phi(r,t)$ for time $(n+\frac{1}{2})\Delta t$, to be obtained by an iterative procedure described below. If the $\Phi^{n+1/2}$ are available, equation (11) gives the unknowns Ψ^{n+1} explicitly at all net points, except that if $(i+1,j)$ denotes the left-most point on the j^{th} horizontal line, inside the semicircle, like the point B_1 in figure 2, the quantity $\Psi^{n}_{i,j}$ needed in (11) is not available. But the boundary condition says that Ψ vanishes at point P_1 of space-time at which the trajectory through $(i+1,j,n+1)$ enters the system, at radius a. In this case we replace Δx in (11) by $\sqrt{a^2-y_j^2} - x_{i+1}$, which is the distance from the point $(i+1,j)$ to the boundary along the line $y = y_j$; we also replace $\Psi^{n}_{i,j}$ by zero; then (11) gives $\Psi^{n+1}_{i+1,j}$ as for other net points in the system.

To explain more fully the treatment of exceptional points, we refer to figure 2, which is a perspective drawing showing certain features of the three-dimensional net. The line segments A_1B_2, A_2B_3, etc. are trajectories or characteristics connecting net points at time t^n with those at time t^{n+1}. The quantity $\Phi^{n+1/2}(r_{i+1/2,j})$ in equation (11) represents generally an average value of $\Phi(r,t)$ along such a segment and is taken as the average value of Φ at the two ends of the segment. For a segment like A_1B_2 this

involves a value of $\Phi^n(r)$ at one end and of Φ^{n+1} at the other.

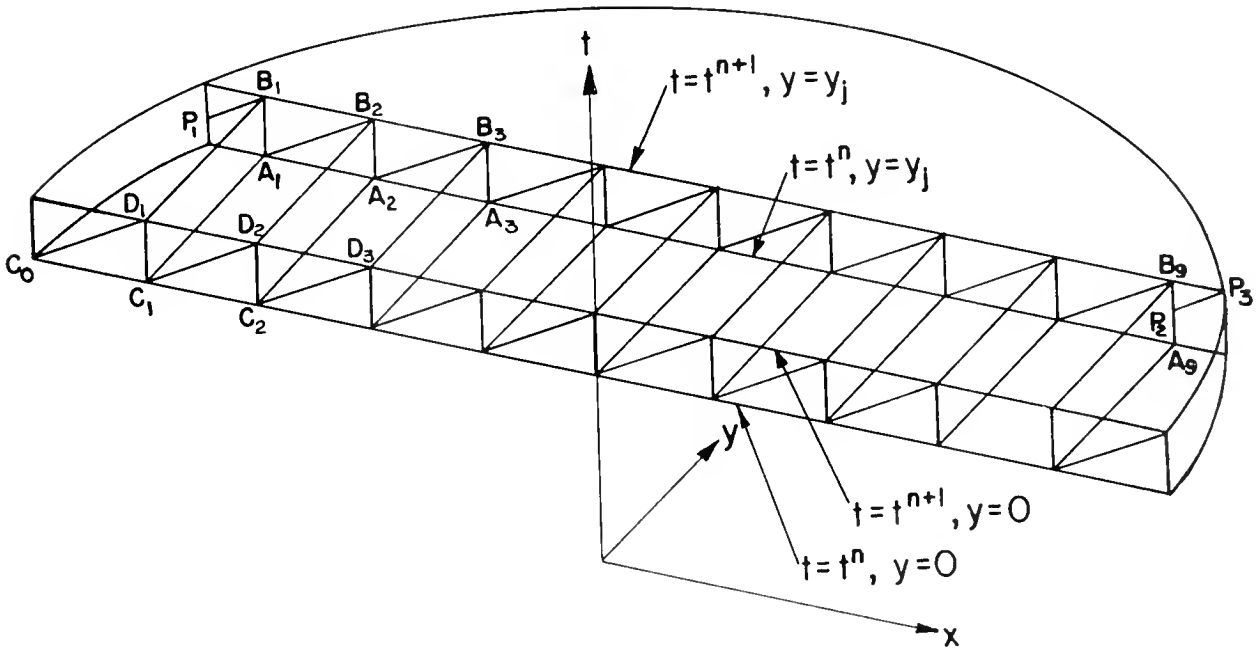

Figure 2

The special short segments like P_1B_1 and P_2P_3 require a modification of the procedure. These segments terminate on the plane $t = t^{n+1}$ but originate at points, namely P_1 and P_2 respectively, which lie between the planes $t = t^n$ and $t = t^{n+1}$. We first obtain a value of Φ at the early end of such a segment by linear interpolation in time; then the quantity $\Phi^{n+1/2}$ in equation (11) is taken as the average of the values of Φ at the two ends of the segment. For example, in the equation to determine Ψ^{n+1} at point P_3 (see figure 2), the right hand side of (11) is taken as

$$\sigma \frac{1+f}{4\pi} \left[\frac{1}{2} \Phi(P_2) + \frac{1}{2} \Phi(P_3)\right] ,$$

where $\Phi(P_2)$ has been obtained in turn by linear inter-

polation between $\Phi(A_j)$ and $\Phi(B_9)$. The net result is that $\Phi^{n+1/2}(r_{i+1/2,j})$ in equation (11) has been interpreted as a value obtained by two-way interpolation (with respect to x and t) among the values of Φ at points A_0, B_9 and P_3 to give an approximation to Φ at the midpoint of the segment P_2P_3.

A further refinement of this equation (the equation to determine Ψ^{n+1} at point P_3) is that Ψ^n_{ij} in the left-hand member is similarly replaced by $\Psi(P_2)$ which is a value obtained by linear interpolation between $\Psi(A_9)$ and $\Psi(B_0)$ -- that is, between Ψ^n_{ij} and Ψ^{n+1}_{ij}. (This requires that the equations be solved in order of increasing i, so that Ψ^{n+1}_{ij} will be available when we are computing $\Psi(P_3)$). Lastly Δx is replaced by the distance between the points B_9 and P_3 -- i.e. by $\sqrt{a^2-y_j^2} - x_1$.

When the $\Psi^{n+1}_{i,j}$ are known at all net points, the Φ^{n+1}_p are computed. Equation (8) or (9) shows that Φ^{n+1}_p is given by a line integral of Ψ^{n+1} around a semicircle of radius $p\Delta r$ in the x,y plane. Generally this semicircle will pass through few, if any, of the net points, and interpolation is required. The machine calculates Φ^{n+1}_p by applying the trapezoid rule to equation (9), using $\frac{1}{2}\Delta x$ as the increment of x for this purpose and obtaining the values of the integrand at the required abscissas x by linear interpolation with respect to x and y.

The iterative procedure for solving (11) is as follows: At the beginning of a complete cycle of the calculation, the $\Psi^n_{i,j}$ are known and a table of Φ^n_p is available. The quantity $\Phi^{n+1/2}(r_{i+1/2,j})$ on the right of (11) is first approximated by simply $\Phi^n(r_{i+1/2,j})$, obtained by linear interpolation in the table of Φ^n_p at $r = r_{i+1/2,j}$. Equation (11) is then solved to give preliminary values of $\Psi^{n+1}_{i,j}$. From these, provisional values of Φ^{n+1}_p are obtained by the trapezoid-rule integration described in the preceding paragraph. A second calculation (iteration) is then performed, in which $\Phi^{n+1/2}(r)$ is taken as the mean of $\Phi^n(r)$ and $\Phi^{n+1}(r)$. This iteration results in improved values of $\Psi^{n+1}_{i,j}$, from which improved values of Φ^{n+1}_p are obtained.

Experience indicates that generally further iterations are not worthwhile -- using a finer net pays off more rapidly. This is presumably because the first iteration decreases the truncation error formally from $\mathcal{O}(\Delta t)$ to $\mathcal{O}((\Delta t)^2)$, and further iterations change only the coefficient of the error term but not the power of Δt.

V. The Trial Calculation

The method was applied to a simplified problem of conceivable astrophysical interest but chosen mainly to illustrate the method. It applies to photons rather than neutrons; hence the speed is called c instead of v. A short burst of light (as from a variable star) is emitted at time $t = 0$ from a point source situated at the center of a large homogeneous spherical cloud of purely scattering material ($f = 0$) which is assumed to scatter isotropically and without polarization effects. Required is a curve of intensity vs. time for the light emitted from the cloud.

Several calculations were made for a sphere of 2 mean free paths radius and one calculation for a sphere of 4 mean free paths radius. Some of the results are given graphically in figures 3A, 3B, 4, 5, 6. Choosing the mean free path and mean free time as units of length and time, we have:

Case I $\quad \sigma = 1, \quad v = c = 1, \quad a = 2.$

Case II $\quad \sigma = 1, \quad v = c = 1, \quad a = 4.$

In the first two attemps to calculate case I ($I = J = 10$, 162 interior net points; and $I = J = 15$, about 350 interior net points), the problem was treated in a straightforward way as an initial-value problem: at $n = 0$ ($t = 0$) Ψ^n_{ij} was set equal to zero except at the central net point

$i = j = 0$, where it was arbitrarily set equal to 0.1. The photons were thus initially concentrated into the immediate neighborhood of the point source and then allowed to move in accordance with the transport equation. This treatment was unsuccessful, except in a rough, qualitative way, because of the violently discontinuous nature of the distribution at early times. Spreading out the initial distribution over 3 or 4 net points was also tried, but produced little improvement.

The procedure was then modified as follows: Ψ_{ij}^{n} was taken identically zero for $n = 0$, and a source term was introduced into the transport equation during the interval $0 \leq t \leq a/c$ while the initial light-pulse from the star was travelling outward through the sphere, the source being located at position $r = ct$ at time t and representing photons emerging from their first scattering collision. In other words, the first collision was treated analytically and subsequent ones by the numerical calculation. The initial pulse travels out as an expanding spherical shell with a number of photons per unit area of the shell proportional to $e^{-\sigma r}/r^2$. To allow for a shell source proportional to this, it is necessary only to add the quantity $Ae^{-\sigma p \Delta r}/p^2$ to Φ_p^{n+1} after the cycle for which $n+1 = p$. Before the first cycle Φ_o^o was set equal to a value chosen to represent approximately the photons injected into the system by the shell source during the time-interval $(0, \frac{1}{2}\Delta t)$ (the other Φ_p^o were

zero). The constant A was taken proportional to I^3 so that when a problem was rerun with a finer net the total number of photons introduced during the interval $(0,a/c)$ should be the same. The number of photons introduced in the p^{th} cycle by our procedure is proportional to

$$\delta\Phi_p r^2 \Delta r \Delta t = \delta\Phi_p (p\Delta r)^2 \Delta r \frac{\Delta r}{c} =$$

$$= \delta\Phi_p \frac{p^2}{c} \left(\frac{a}{I}\right)^4$$

where $\delta\Phi_p = Ae^{-\sigma p \Delta r}/p^2$. The total number introduced is proportional to

$$\sum_{(p)} Ae^{-\sigma p \Delta r} \cdot \left(\frac{a}{I}\right)^4 \approx A \int_0^a e^{-\sigma r}\, dr \left(\frac{a}{I}\right)^3 .$$

With this modification the functions Φ and Ψ which one is trying to compute still have discontinuities during the time interval $(0,a/c)$, but at least they are bounded and do not require Dirac delta-functions for their representation.

The emergent flux F at $r = a$ was obtained by trapezoid-rule evaluation of the integral in the equation:

$$F = 2\pi \int_0^{\pi/2} \sin\vartheta\, d\vartheta\, \Psi(a\cos\vartheta,\ a\sin\vartheta, t).$$

The flux F is shown plotted on a logarithmic scale as function of t for case I in figure 3a and for

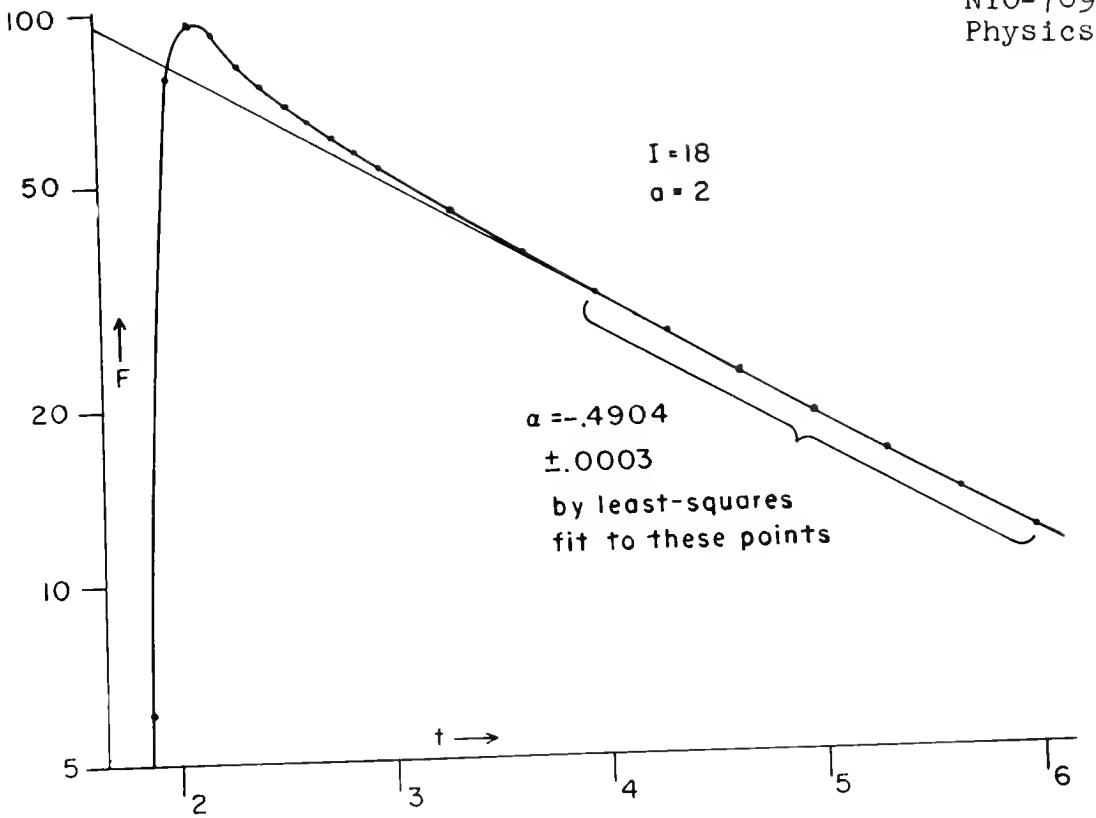

Figure 3a

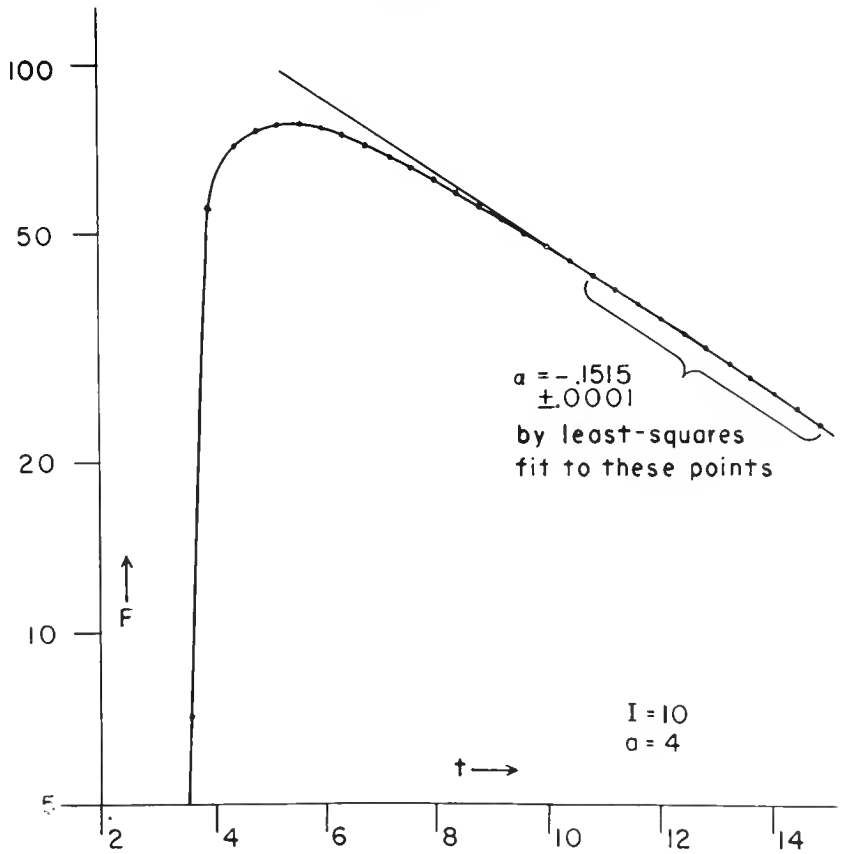

Figure 3b

case II in figure 3b. In both cases F is practically zero (as it should be) until the instant $t = a/c$ when the original pulse emerges. Thereafter the cloud shines with an intensity which varies with time as shown. At first the curve of F vs. t shows a transient behavior, but later it settles down to a very nearly exponential decline.

The spatial density $\Phi = \Phi(r,t)$ is shown as function

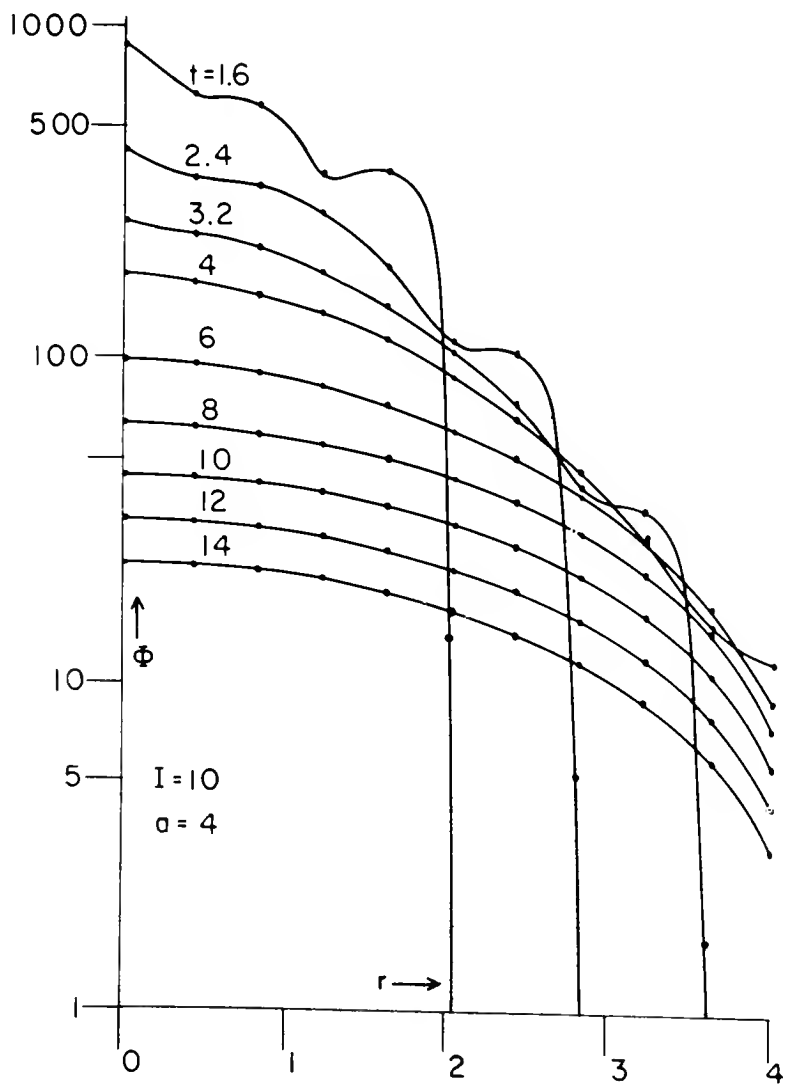

Figure 4

of r at various times t for case II in figure 4. In the three earliest curves the discontinuous radiation front at $r = ct$ is clearly visible. The oscillations behind the front are presumably spurious, having been somehow introduced by the truncation error of the finite difference equations. After the instant $t = a/c = 2$, the distribution is quite smooth and settles down to a steady shape.

We have no exact information with which to compare these results but one can get an idea of the accuracy attained in various indirect ways. In the first place there are several internal checks which can be applied to the calculation. For example, the total number N of photons in the cloud at an instant t can be obtained either as the space integral of the space density:

$$N = N_1 = 4\pi \int_0^a r^2 \, dr \, \Phi(r) \quad ,$$

or as the phase space integral of the phase space density:

$$N = N_2 = 2\pi \iint dxdy \; y \; \Psi(x,y) \quad ,$$

this last integral being extended over the semicircular region: $x^2 + y^2 \leq a^2$, $y > 0$. N_1 and N_2 should of course be equal. After each cycle the machine evaluated N_1 and N_2 (essentially by the trapezoid rule) and printed them out. During the interval $0 \leq t \leq a/c$, while

the discontinuous front was moving outward, there was generally a quite large discrepancy between N_1 and N_2 but later the agreement was better. For the calculation shown in figure 3a, the difference between N_1 and N_2 was approximately:

$$15\% \qquad \text{at} \quad t = \tfrac{1}{2}\, a/c = 1$$

$$3\% \qquad \text{at} \quad t = a/c = 2$$

$$1.6\% \text{(average) for } a/c < t < 2a/c \quad (\text{i.e. for } 2 < t < 4)$$

Considering the small number of net points used (18 on the radius), this discrepancy is perhaps not surprising. Furthermore there is some evidence that even this discrepancy was due in part to poor scaling (loss of significant figures) rather than truncation error, for the portion $2\,\frac{a}{c} \le t \le 3\,\frac{a}{c}$ of the calculation was performed after rescaling, and the average discrepancy between N_1 and N_2 was only 0.4 % for $2\,\frac{a}{c} \le t \le 3\,\frac{a}{c}$.

As a second internal check, the quantity

$$T = N + \int F dt$$

should be constant, by conservation of photons, for $t > a/c$; i.e., after the source term is no longer present in the equation. If N_2 is used for N in the above equation, it is found that T is indeed quite constant; the average deviation of T from its mean value for $a/c < t / 2\ a/c$

was 0.11% for the calculation shown in figure 3a. This suggests, incidentally, that N_2 (integration over phase space) provides a better estimate of N that does N_1 (integration over space).

A second type of check on the accuracy resulted from varying the net spacing. The calculation was also performed with a coarser net than used for figure 3a; $I = 12$ instead of $I = 18$. The results agreed well with the ones shown, except in the immediate vicinity of $t = a/c$, where the sudden onset of the luminosity was slightly less abrupt than for $I = 18$. For $t > a/c$, the two curves have the same shape to an accuracy of about 0.5%, but the one for $I = 12$ is consistently about 2.5% lower than that for $I = 18$.

VI. The Asymptotic Form

Further evidence of the accuracy of the method comes from the asymptotic behavior of the solution for large values of t. The normal mode expansion (5) indicates that for sufficiently large t the fundamental mode (the mode with the highest value of α) should predominate. Therefore the asymptotic form is

$$\Psi(x,y,t) = \Psi^{(o)}(x,y)e^{\alpha^{(o)}t} \quad ,$$

$$\Phi(r,t) = \Phi^{(o)}(r)e^{\alpha^{(o)}t} \quad .$$

If these expressions are substituted into the transport equation, the resulting equation (which then has the character of an ordinary differential equation for fixed y if $\Phi^{(o)}$ is regarded as known) can be solved for $\Psi^{(o)}$ in terms of $\Phi^{(o)}$. If the result is substituted into the equation (8) defining $\Phi^{(o)}$, one obtains an integral equation for $\Phi^{(o)}(r)$, which can be put into the form

$$\lambda\Phi^{(o)}(r) = \frac{1}{2}\int_{-a}^{a} E((\sigma + \frac{\alpha_o}{v})|s-r|)\Phi^{(o)}(s)ds \qquad (12)$$

where

$$\lambda = (\sigma(1 + f))^{-1}$$

and

$$E(x) = \int_{x}^{\infty} \frac{e^{-y}dy}{y}$$

$\Phi^{o}(r)$ is in fact that odd solution of (12) corresponding to the largest eigenvalue λ. (To derive (12) one must assume that σ is constant: in our calculation, f was also constant; namely, f = 0).

The numerical method of solving (12) that was used will be described in the next section. The procedure is more or less standard and so accurate that the results may be regarded as exact for purposes of comparison with those described in the preceding section.

Examination of the numerical solution shown in figure 3a shows that for $2\frac{a}{c} < t < 3\frac{a}{c}$ the decay is quite accurately exponential and the value of the decay constant is $\alpha = -.4904$, from the slope of the graph, by least-squares fit to the last few points, as shown in the figure. We therefore suppose that the asymptotic form of the solution has been fairly well established by $t = 2\frac{a}{c}$ and we compare this form with the correct one as given by the integral equation method. The correct value of α is $\alpha = -.4925$, from which our value differs by less than 1/2%. In figure 6 the radial dependence of $\Phi(r,t)$ for $t = 2.5\frac{a}{c}$ (from one of the early calculations) is compared with the fundamental solution $\Phi^{(o)}(r)$ of (12), suitably normalized. The discrepancy is within 1%, except for the point on the surface, r = 2, where it is where it is 5%.

Similarly, a least-squares fit gives $\alpha = -.1515$ for a sphere of 4 mean free paths radius ($a = 4$), as compared with the correct value of $\alpha = -.1529$ from the integral equation.

VII. Iterative Solution of the Integral Equation

In writing the integral equation (12) we have followed the procedure that is customary in this work, of defining $\Phi^{o}(r)$ for negative r as $-\Phi^{o}(-r)$ to simplify the form of the result. For the numerical work it is more convenient to work with the range $0 \leq r \leq a$. Recalling that $f = 0$, and taking units such that $\sigma = 1$, $v = 1$, we have

$$\lambda\Phi(r) = \int_{o}^{a} K_{\alpha}(r,s)\, \Phi(s)ds \qquad 0 \leq r \leq a \tag{13}$$

where

$$K_{\alpha}(r,s) = \frac{1}{2}\left[E((1+\alpha)|r-s|) - E((1+\alpha)|r+s|)\right]. \tag{14}$$

The superscript "(o)" has also been dropped from $\Phi(r)$.

For any real $\alpha > -1$, $K_{\alpha}(r,s)$ is a symmetric kernal of Hilbert-Schmidt type (non-degenerate)*. It can also be shown to be positive definite. Therefore the eigenvalues of (13) form a positive sequence $\lambda_{o} \geq \lambda_{1} \geq \lambda_{2} \cdots$ tending to zero; each is of finite multiplicity; and the corresponding eigenfunctions may be taken as an orthonormal set over the interval $(0,a)$. Furthermore, since

---

* For the general theory of such integral equations see Courant-Hilbert, Methods of Mathematical Physics, Chapter III. The extensions of the theory necessitated by the singularity of the kernel $K_{\alpha}(r,s)$ at $r = s$ are described in section 9 of that chapter.

the kernel $K_\alpha(r,s)$ is positive for $0 \leq r \leq a$, $0 \leq s \leq a$, the highest eigenvalue λ_o is of multiplicity 1, so $\lambda_o > \lambda_1$, and the corresponding eigenfunction $\Phi(r)$ is of one sign (and may be taken as ≥ 0) throughout the interval $(0,a)$. The eigenfunctions corresponding to $\lambda_1, \lambda_2, \cdots$ will be denoted by $X_1(r)$, $X_2(r)$, etc.

The problem is to find a value of α such that the highest eigenvalue of (13), λ_o, is exactly $= \sigma^{-1} = 1$, and then to find the corresponding eigenfunction $\Phi(r)$. If one has a general procedure for finding the largest eigenvalue and corresponding eigenfunction of an equation like (13) for any given value of α, then it is only necessary to include a trial-and-error method of adjusting α until $\lambda_o = 1$.

The well-known iterative procedure for finding the largest eigenvalue is the following: Let $h(r)$ be an arbitrary positive continuous function for $0 \leq r \leq a$, and define

$$g_o(r) = h(r)$$

$$g_p(r) = \int_o^a ds K_\alpha(r,s) g_{p-1}(s)$$

$$p = 1,2,3, \cdots$$

$$a_p = \left\{ \int_o^a ds [g_p(s)]^2 \right\}^{1/2}$$

$$p = 0,1,2, \cdots$$

Clearly a_p is just the reciprocal of the normalizing factor for $g_p(r)$. According to the general theory any function that can be written as $\int K_\alpha(r,s)h(s)ds$, with some continuous $h(s)$, can be expanded in the eigenfunctions. This applies to $g_1(r)$, $g_2(r)$, etc. Therefore,

$$g_1(r) = c_o\Phi(r) + c_1X_1(r) + c_2X_2(r) + \cdots,$$

$$g_{p+1}(r) = c_o\lambda_o{}^p(r) + c_1\lambda_1{}^pX_1(r) + c_2\lambda_2{}^pX_2(r) + \cdots,$$

and

$$a_{p+1} = \left\{ c_o{}^2\lambda_o{}^{2p} + c_1{}^2\lambda_1{}^{2p} + c_2{}^2\lambda_2{}^{2p} + \cdots \right\}^{1/2}$$

On dividing *, it is seen that

$$\frac{g_{p+1}(r)}{a_{p+1}} = \Phi(r) + \cdots,$$

where the dots indicate terms containing factors

$$\left(\frac{\lambda_1}{\lambda_o}\right)^p, \left(\frac{\lambda_1}{\lambda_o}\right)^{2p}, \cdots \left(\frac{\lambda_2}{\lambda_o}\right)^p, \left(\frac{\lambda_2}{\lambda_o}\right)^{2p}; \cdots, \text{ etc.}$$

Since $\lambda_o > \lambda_1 \geq \lambda_2 \geq \cdots$, all these terms vanish in the limit as $p \to \infty$. That is,

$$\lim_{p\to\infty} \frac{g_p(r)}{a_p} = \Phi(r).$$

---

*c_o cannot vanish, because $h(r) > 0$, therefore $g_1(r) > 0$, therefore $c_o = \int g_1(r)\Phi(r)dr > 0$ because $\Phi(r) > 0$.

Similarly, $\lim_{p\to\infty} \frac{a_{p+1}}{a_p} = \lambda_o$.

VIII. Improved Iterative Method

There are many well-known schemes for accelerating the convergence of this iterative procedure, and the one used in our calculation* is the following. Let $\mu_1, \mu_2, \cdots \mu_N$ be N real constants, whose values are to be decided on later. Given a function $g_p(r)$, we define

$$g_{p+1}(r) = \int_o^a K_\alpha(r,s) g_p(s) ds - \mu_1 g_p(r)$$

$$g_{p+2}(r) = \int_o^a K_\alpha(r,s) g_{p+1}(s) ds - \mu_2 g_{p+1}(r) \tag{15}$$

$$\vdots$$

$$g_{p+N}(r) = \int_o^a K_\alpha(r,s) g_{p+N-1}(s) ds - \mu_N g_{p+N-1}(r).$$

Then if $g_p(r)$ is of the form $\int_o^a K_\alpha(r,s)h(s)$ for some $h(s)$ we can again expand:

$$g_p(r) = c_o \Phi(r) + c_1 X_1(r) + \cdots$$

and clearly

$$g_{p+N}(r) = c_o F(\lambda_o)\Phi(r) + c_1 F(\lambda_1) X_1(r) + \cdots$$

where $F(\lambda)$ is the polynomial

$$F(\lambda) = (\lambda-\mu_1)(\lambda-\mu_2)\cdots(\lambda-\mu_N).$$

---

*essentially that of Flanders and Shortley, J. Appl. Phys. vol. 21, p. 1326 (1950).

What is desired is to choose the $\mu_1, \cdots, \mu_N$ so as to make the ratios $F(\lambda_1)/F(\lambda_o)$, $F(\lambda_2)/F(\lambda_o)$, etc., all as small as possible. We can achieve essentially this by use of Tchebycheff polynomials*, if we know the value of the second eigenvalue, λ_1, for then all the eigenvalues except λ_o lie in the interval $(0,\lambda_1)$, and

$$F(\lambda) = T_N(2\frac{\lambda}{\lambda_1} - 1)$$

is, as is well-known, the polynomial of degree N for which

$$\underset{0\leq\lambda\leq\lambda_1}{\text{Max}} \; |F(\lambda)|$$

is as small as possible, for given leading coefficient. $T_N(z)$ is the Tchebycheff polynomial defined by

$$T_N(z) = \frac{1}{2^{N-1}} \cos\,(N \cos^{-1} z).$$

The zeros of $T_N(z)$ are clearly at

$$z = \cos \frac{2\ell-1}{2N}\pi \quad , \qquad \ell = 1, 2, \cdots, N \, ,$$

and therefore we take

$$\mu_\ell = \frac{\lambda_1}{2}\,(1 + \cos \frac{2\ell-1}{2N}\pi), \quad \ell = 1, 2, \cdots, N. \tag{16}$$

Since λ_1 is not known in advance, we use an approximate value of it which is improved as the calculation

---

*see Courant-Hilbert, ibid, Chapter II, section 9, part 2.

proceeds, by a calculation of λ_1 and the eigenfunction $X_1(r)$ that proceeds concurrently with the calculation of λ_o and $\Phi(r)$. The calculation of $X_1(r)$ is similar to that of $\Phi(r)$, except that it is necessarily somewhat less refined, because we assume no knowledge whatever of λ_2. After each set of N iterations (15) for improvement of $\Phi(r)$, a set of M similar iterations is performed for improvement of $X_1(r)$. These are of the same form as (15); viz.,

$$(17)\quad \begin{cases} k_{p+1}(r) = \int K_\alpha(r,s)k_p(s)ds - \nu_1 k_p(r) \\ \qquad\qquad \vdots \\ k_{p+M}(r) = \int K_\alpha(r,s)k_{p+M-1}(s)ds - \nu_M k_{p+M-1}(r) \end{cases}$$

except that the constants ν_1 are now chosen as

$$\nu_1 = \lambda_o$$

$$\nu_2 = \nu_3 = \cdots = \nu_M = 0$$

(the value of λ_o used here is the estimate obtained from the preceding N iterations to improve $\Phi(r)$). The corresponding polynomial, $G(\lambda) = (\lambda-\nu_1)(\lambda-\nu_2)\cdots(\lambda-\nu_M)$ is then simply $(\lambda-\lambda_o)\lambda^{M-1}$. It vanishes at $\lambda = \lambda_o$, and if one is lucky in the choice of M it will have a maximum near $\lambda = \lambda_1$ and be quite small for $\lambda = \lambda_2$, etc. (If one does not wish to count too much on luck, it is better to have M too large than too small). The corresponding functions $k_p(r)$ approach $X_1(r)$, for $p \to \infty$, as orthogonality to $\Phi(r)$ is assured in the limit because $G(\lambda_o) = 0$.

After each set of N iterations on $\Phi(r)$ and M iterations on $X_1(r)$, the value of α is adjusted automatically in such a direction as to bring λ_o closer to 1. To do this, the machine remembers the last two values of α used, say α' and α'', and the corresponding approximations λ_o' and λ_o'' to λ_o. It then takes as the next trial value the quantity

$$\alpha = \frac{\alpha''(1-\lambda_o')+\alpha'(\lambda_o''-1)}{\lambda_o''-\lambda_o'} \quad . \tag{18}$$

The machine then prints out the values of α and of λ_1 obtained so far, computes the new kernel $K_\alpha(r,s)$ (in partially integrated form as described below), and proceeds with the next iteration. The iterations may be stopped (on a breakpoint) whenever desired: the values of $\Phi(r)$ and $X_1(r)$ are then available on magnetic tapes.

IX. The Numerical Procedure for Solving the Integral Equation

The integration is performed numerically after integration by parts to remove the singularity of the kernel $K_\alpha(r,s)$ at $r = s$. That is, we set

$$\Delta x = a/J, \qquad (J = \text{integer});$$

then, in order to evaluate an integral of the form

$$f(x) = \int_o^a K_\alpha(x,y)\,\varphi(y)\,dy$$

we write

$$f_{i+1/2} = \sum_o^{J-1}(j)\left[\int_{j\Delta x}^{(j+1)\Delta x} K_\alpha(x_{i+\frac{1}{2}},y)\,dy\right]\varphi_{j+\frac{1}{2}} \tag{19}$$

where $f_{i+1/2}$ is an abbreviation for $f((i+1/2)\Delta x)$, and $\varphi_{j+1/2}$ for $((j+1/2)\Delta x)$. The quantity in the square bracket is a coefficient depending on i and j: it can be computed in terms of the function

$$g(x) = \int_o^x E(y)\,dy\ ,$$

a table of which has been computed in advance by a special routine and is available on tape.

At the beginning of the routine there is an opportunity for the operator to type in values of J (the number of net points), of N and M (the numbers of iterations of each kind) and of a (the radius of the sphere in mean free paths). The machine then generates

some rather crude trial functions (sinusordal) $\Phi(r)$ and $X_1(r)$ and then goes into the iterative routine.

To illustrate: with $J = 40$, $N = M = 3$, $a = 2.0$, the successive iterations gave values in the following table:

α	λ_1
-.367	
-.500	.521
-.4923	.522
-.4925	.5223
-.49250	.5222
-.49249	.52222
-.492482	.522210

The convergence is seen to be quite rapid; (we have given only those digits that seem relevant). To test the effect of changing the interval size Δx, a second run was made with $J = 20$ instead of 40. This gave a similar sequence of numbers appearing to tend asymptotically to the values

$$\alpha = -.49252 \quad , \quad \lambda_1 = .52168$$

It was on the strength of these results that we took $\alpha = -.4925$ in section VI.

The functions $\Phi(r)$ and $X_1(r)$ obtained for $J = 40$ are shown graphically in figure 7.

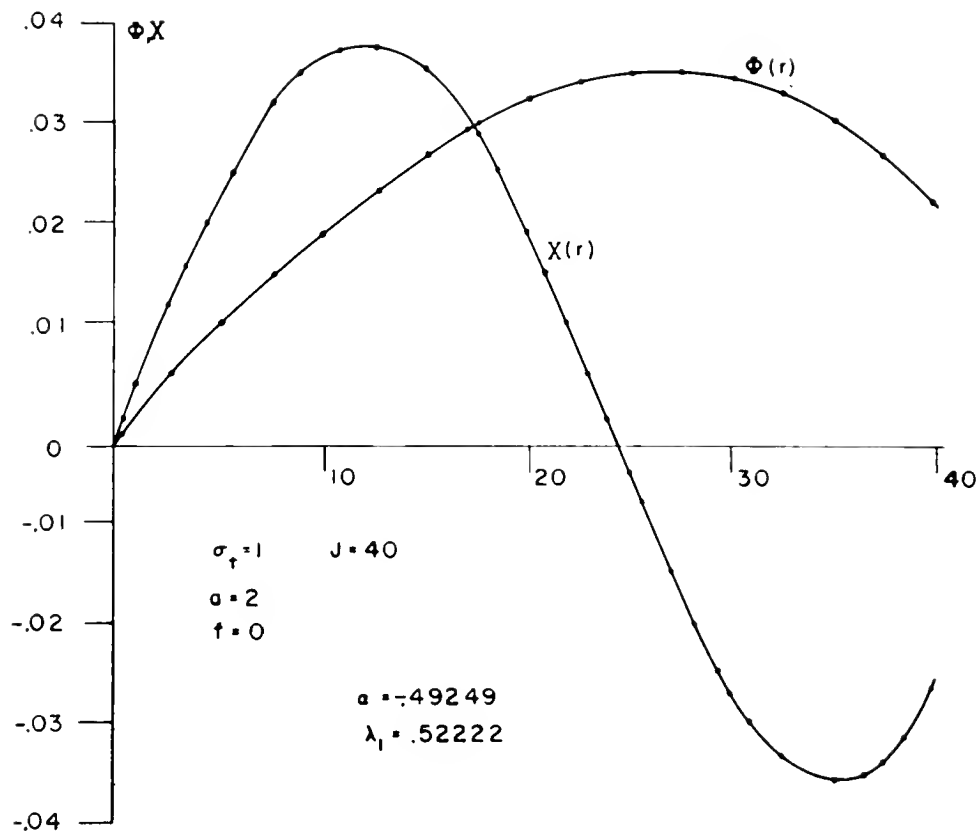

Figure 7

In another series of calculations, for a sphere of 4.0 mean free paths radius, i.e. with a = 4.0, the asymptotic values were

J = 20	α = -.15316	λ_1 = .7357
J = 40	α = -.15293	λ_1 = .7364
J = 60	α = -.15289	λ_1 = .7369

X. List of Machine Routines

A. "Ei" routine computes a table of the function

$$10^{-1}g(x) = 10^{-1}\int_0^x E(y)dy$$

from series expansions and other known formulas, and writes a table, at arguments:

$$x = 0 - 1.04 \quad (.02),$$
$$x = 1 - 5.2 \quad (.1),$$
$$x = 5 - 26 \quad (.5),$$

in three consecutive blocks on a magnetic tape. The degree of overlap was designed to facilitate quadratic interpolation. There is no input.

B. "Eep" routine prepares the preliminary trial values of $\Phi(r)$ and $X_1(r)$ and an estimate of α based on slightly modified diffusion theory. Input: a,J.

C. "Milne" routine computes the coefficients in formula (19) for the numerical integration from the given value of α and the table of $g(x)$, and performs the iterations (15) and (17) described above. For the first two sets of iterations α is taken as $0.9\alpha_o$ and $1.1\alpha_o$ where α_o is the preliminary estimate of α obtained in the "Eep" routine. After that, equation (18) is always used

to obtain the new α. Input: N (M is taken = N by this routine).

D. "Transport eqn. coef. gen." prepares in advance and writes on tape two sets of coefficients; one for interpolating among the tabulated values Φ_p^n to obtain $\Phi^n(r_{i+1/2,j})$ and one for the double interpolations among the $\Psi_{i,j}^n$ needed in computing the integral expression for $\Phi(r)$ by equation (9). The ability to precompute these coefficients and read them from tape as needed without loss of computing time proved to be a marked improvement of the present code over the Los Alamos Maniac code, which had been prepared before the magnetic drum was available on that machine. Input: I (the routine takes J = I).

E. "Transport eqn. main" (mod 2): performs the calculation described in section IV, modified as described in section V. After each cycle a table of Φ_p^{n+1} and values of various integral quantities are printed on the supervisory control printer. Various breakpoint options are available: e.g. to increase or decrease

the number of iterations; to write a complete table of $\Psi^{n+1}(x,y)$ at any desired cycle from the working tapes onto another tape where it can be saved for subsequent printing. Three working tapes are used: in any cycle one is being read, one is being written on, and one is idle (to make reruns possible): The three are permuted cyclically after each complete cycle. A memory dump is made every cycle for reruns. Input: a (radius of sphere in mean free paths).

2479

NYU
NYO-
7696 Richtmyer

A numerical method for

the time-dependent.....

NYU 2479
NYO-
7696

Richtmyer
A numerical method for the
time-dependent transport equati
ion.

Date Due

PRINTED IN U. S. A.